GEOPHYSICAL RESEARCH LETTERS, VOL. 36, L15815, doi:10.1029/2009GL038026, 2009

Very high resolution precipitation climatologies from the Tropical Rainfall Measuring Mission precipitation radar

Stephen W. Nesbitt[1] and Alison M. Anders[2]

Received 4 March 2009; revised 6 July 2009; accepted 13 July 2009; published 8 August 2009.

[1] To investigate processes related to the interaction of topography and precipitation, a tropics-wide (±36° latitude) high resolution (0.1°) ten year (1998–2007) rainfall climatology is presented from the Tropical Rainfall Measuring Mission (TRMM) precipitation radar (PR) using algorithm 2A25 version 6 near-surface rain. We observe a tight coupling between precipitation and topography with distinct precipitation-topography relationships present in northwest South America and South Asia. An error model is developed by subsampling the TRMM Multi-satellite Precipitation Analysis as sampled by the PR. The error model predicts observed sampling error as a function of resolution, rain rate and sampling frequency with an r^2 of 0.82. This error model indicates that the precipitation climatology at 0.1° resolution does resolve precipitation gradients in regions with large average daily rain totals including the Andes, Western Ghats, and Himalaya. **Citation:** Nesbitt, S. W., and A. M. Anders (2009), Very high resolution precipitation climatologies from the Tropical Rainfall Measuring Mission precipitation radar, *Geophys. Res. Lett.*, *36*, L15815, doi:10.1029/2009GL038026.

1. Introduction

[2] Spatial gradients in precipitation are a striking feature of mountain climates. Variability of a factor of 2–10 in annual precipitation totals over spatial scales of several to tens of kilometers is common in steep topography. Understanding orographic precipitation processes requires addressing this extreme variability in precipitation, which is increasingly recognized as a key component of the topographic and geologic evolution of mountain ranges over long timescales. However, precipitation in mountainous regions remains poorly constrained due to the difficulty of measuring precipitation in steep topography - whether by direct gauging of rain and snow, or with remote sensing techniques. In particular, the variability in precipitation in mountainous regions makes point measurements with gauges likely to miss important structures in the precipitation field. Ground-based radar is blocked by topography, preventing measurement of near-surface precipitation rates. Additionally, the coarse spatial resolution and retrieval uncertainties of passive remote sensing do not allow for depiction of small-scale gradients in precipitation.

[3] The Tropical Rainfall Measuring Mission (TRMM) has revolutionized our global view of precipitation in many ways. In particular, the precipitation radar (PR) of the TRMM satellite provides a unique high spatial resolution measurement of precipitation and an ability to profile the vertical structure of precipitation. The PR is an active sensor, providing through the well-developed 2A25 retrieval algorithm [*Iguchi et al.*, 2000] arguably the most reliable over-land precipitation detection and rate determination at the highest spatial resolution (~4–5 km) of any of TRMM's sensors. A low earth orbit with an inclination of 35° means that TRMM measures precipitation relatively infrequently at any single location, leading to non-negligible sampling error [*Bell and Kundu*, 1996]. However, with the collection of more than a decade of data since TRMM's launch on 29 November 1997, the possibility of creating rainfall climatologies at much higher spatial resolution now presents itself.

[4] High-resolution precipitation climatologies (up to 5 km) for use in studies of precipitation-land-surface interactions have been generated from the PR [*Anders et al.*, 2006; *Barros et al.*, 2004; *Kidd and McGregor*, 2007] and combined PR-passive microwave algorithm 2B31 [*Bookhagen and Burbank*, 2006; *Bookhagen and Strecker*, 2008]. The shorter time records used in these studies indicate that sampling errors are larger than in this study, and the majority of these studies did not address sampling or retrieval errors. The TRMM 2B31 algorithm has comparable sampling errors to 2A25 at high spatial resolutions and has additional factors related to complications in interpreting microwave precipitation estimates over land, and a land-ocean discontinuity in the algorithm [*Haddad et al.*, 1997]. In studies of microphysical processes in orographic precipitation, the climatology of precipitation, and landscape evolution over geomorphically relevant timescales (thousands to millions of years), the need for delineation of spatial gradients in precipitation at scales over which topography varies on meso-α scales (i.e., a few kilometers) far outweighs the need for precise determination of precipitation rates. We examine the feasibility of generating a ten year high resolution precipitation climatology from the PR and present it as a useful tool in both earth-atmosphere interaction studies and investigations atmospheric precipitation processes. We hypothesize that in mountainous regions the strong and persistent gradients in precipitation will be sufficiently large that the signal as recorded by 2A25 over ten years will be resolvable at spatial scales down to ten km.

2. Data and Methods

[5] The TRMM satellite carries several sensors in addition to the PR; we suggest that the PR (product 2A25), being derived from a single, active instrument, is most suitable for generating a high-resolution precipitation cli-

[1]Department of Atmospheric Sciences, University of Illinois at Urbana-Champaign, Urbana, Illinois, USA.
[2]Department of Geology, University of Illinois at Urbana-Champaign, Urbana, Illinois, USA.

0094-8276/09/2009GL038026$05.00

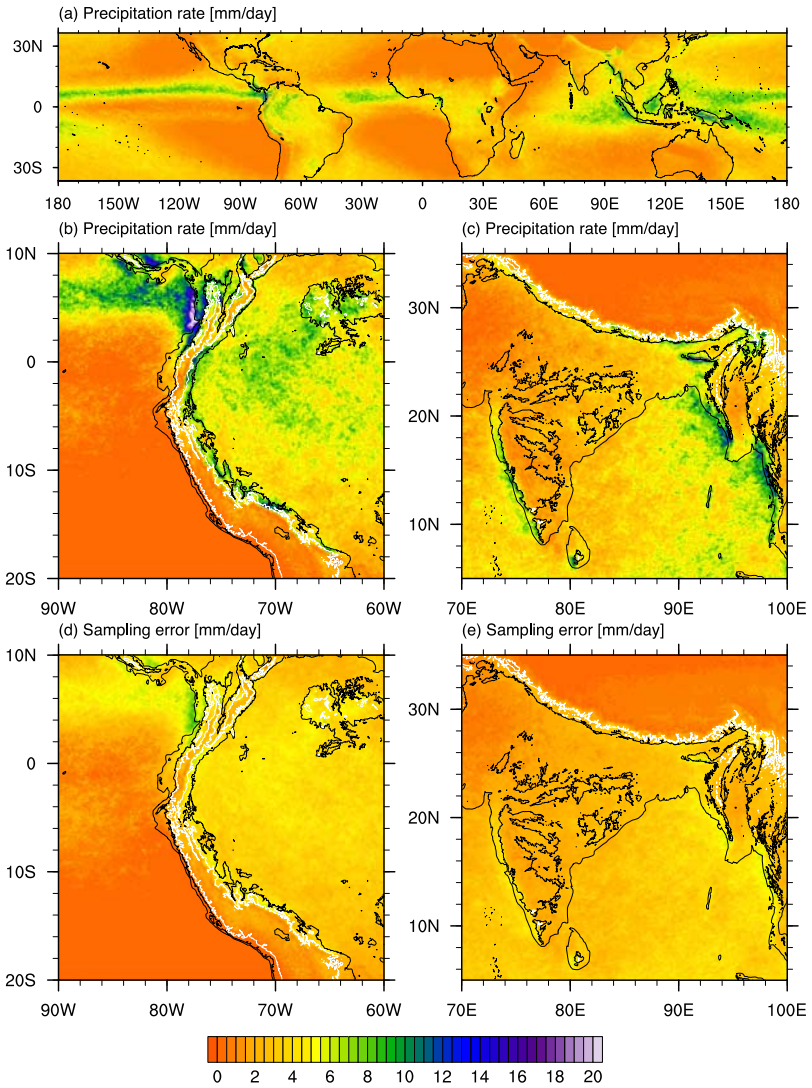

Figure 1. (a) Global view of the TRMM PR 1998–2007 precipitation climatology at 0.1° resolution. Regional enlargements of Figure 1a over (b) northwest South America and (c) south Asia, (d and e) with sampling error predicted by equation (3) in these regions. Topographic contours at 500 and 2000 m elevation are shown in Figures 1b–1e with light black and white lines, respectively.

matology. TRMM provides a 0.25° 3 hourly research-quality rainfall estimate (the TRMM Multi-Sensor Precipitation Analysis or TMPA, or 3B42), which combines PR, multi-satellite passive microwave, and geostationary infrared rainfall estimates every 3 hours, adjusted with monthly rain gauge totals over land [*Huffman et al.*, 2007]. While the sampling error of this estimate is much lower than from the TRMM PR alone (which overflies a particular location every 1–2 days), the use of less-direct rainfall estimates from passive microwave and infrared sensors (where ice scattering signatures and cold cloud and tend to be spatially larger, and likely displaced climatologically from surface rain areas), and the representativeness of gauges, particularly in mountainous regions, introduces measurement errors that are likely to be non-trivial, particularly at high spatial resolution. While 3B42 is not an instantaneous estimate like the PR, the relatively low sampling error of 3B42 may be useful for studies of sampling error in the PR measurements (see section 5).

[6] The ten year precipitation rain rate and frequency (rain rate > 0) climatology based on TRMM 2A25 "near surface rain" was generated at 0.1° latitude-longitude resolution. Note that PR pixel geolocation errors of up to ten km can occur [*Bilanow and Slojkowski*, 2006]. Each 0.1° box receives roughly 7000 to 31000 visits in ten years, depending on latitude (with a maximum near ±35°, not shown). Thus, a key issue is to address the uncertainty in climatological rainfall estimates given this observation frequency.

3. Results

[7] Figure 1 shows the 10-year averaged rainfall rate measured by the PR at 0.1° resolution. In Figure 1a, the precipitation climatology appears as expected, where precipitation rates exceed 6 mm/day in much of the deep tropical Pacific and Indian Oceans. Dry regions are found in the semi-permanent subtropical high regions centered at

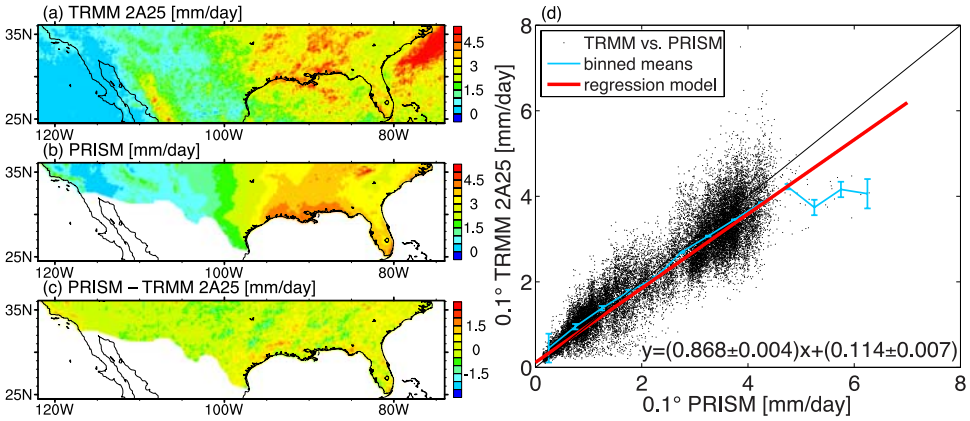

Figure 2. 1998–2007. (a) TRMM PR precipitation rate [mm/day] gridded at 0.1° lat-lon resolution, (b) PRISM precipitation rate [mm/day] gridded at 0.1° lat-lon resolution, (c) PRISM - TRMM [mm/day]. (d) Scatter diagram between TRMM and PRISM, with a least-squares regression line indicated (red line, equation at bottom right), as well as binned histogram means (cyan line, error bars indicate standard deviations).

±15° latitude, where precipitation rates are less than 1 mm/day. Note that this product contains increased noise relative to a lower resolution product. However, if small scale precipitation gradients are of interest, the remainder of this paper will demonstrate that sampling error is acceptable in regions with large gradients in climatological precipitation over short distances.

[8] From Figure 1a, it is evident that striking spatial gradients in this climatology of precipitation rate are found in many coastal and mountainous areas. Adjacent to the wet Amazon basin (Figure 1b), the eastward slopes of the Andes, largely between 500 and 2000 m in elevation contain narrow zones with rain rates > 10 mm/day. A distinctly drier region (with rain rate < 4 mm/day) is found along the high (>2000 m) slopes of the northern Andes and Altiplano to the south. Extremely wet regions are found at low elevations (<500 m to the west of the Cordillera Occidental) where precipitation rates exceed 20 mm/day in the Panama Bight and nearby mountainous coastal region [*Mapes et al.*, 2003].

[9] Over South Asia (Figure 1c), large mesoscale precipitation gradients were found in 0.5° PR data by *Xie et al.* [2006]. Here, we are able to examine remarkable precipitation gradients at meso-α scales. In the Western Ghats range, previous work has investigated an offshore maximum in precipitation [*Grossman and Durran*, 1984; *Smith*, 1985], however, the PR distinctly shows the heaviest precipitation following the meandering 500 m contour for nearly the entire length of the range. Heavy precipitation is also found along the coastal plain possibly due to ascent over near-coast hills or seaward propagating orogenic convective systems [*Ogura and Yoshizaki*, 1988]. Further to the north, the Himalaya displays a double maximum in precipitation, along the southern flank of the foothills at 500 m, as well as the southern flank of the high terrain near 2000 m, with heavier precipitation following the meandering valleys into the range, especially in the east. In the Khasi Hills, despite most rain occurring only during the summer monsoon, rain rates exceed 20 mm/day according to the PR. Precipitation associated with the monsoonally-driven onshore flow near the coast of Burma tends be heaviest below the 500 m contour, with a rain shadow evident in the central Irrawady Valley.

4. Sources of Error

[10] There are several sources of error involved in using the TRMM PR data (2A25) to estimate the climatological precipitation patterns over land. In general, precipitation in mountainous regions is not gauged at resolutions down to 10 kilometers and radars are sparse, especially in the tropics. Additionally, the relationship between precipitation rates at a gauge and average precipitation rates over the footprint of the PR is not straightforward. Therefore, comparisons are limited to interpolated or model-based precipitation analyses. Figure 2 presents the PRISM model, an interpolation of gauge data incorporating elevation and aspect [*Daly et al.*, 1994], for the southern USA and the TRMM climatology for comparison. There is considerable accord as to the shape and location of precipitation gradients in the region, with the PR containing some sampling noise. It is apparent in Figure 2b that the PR has a rain rate-dependent bias relative to PRISM, with the PR higher at low values and low at high values. However, the southern USA lacks strong orographic precipitation gradients observed in many regions in the tropics that would be useful for constraining errors elsewhere.

4.1. Measurement Error

[11] The PR measures radar reflectivity in precipitation at an attenuated wavelength, which must be corrected for *Iguchi et al.* [2000]. Power constraints on a satellite system and the long range to target dictate that the PR is unable to measure the low reflectivities associated with light rain rates below roughly 0.5 mm/hr, and in light snowfall. The conversion of measured radar reflectivity profiles into rain rates is dependent on assumptions about the phase (e.g., snow, mixed-phase, liquid) and particle size distribution. With regards to the latter, the drop size distribution may significantly differ as a function of elevation: rapid conversion of cloud liquid water to precipitation in orographic precipitation may produce a very small mean drop size [*Rosenfeld and Ulbrich*, 2003]. Finally, ground clutter

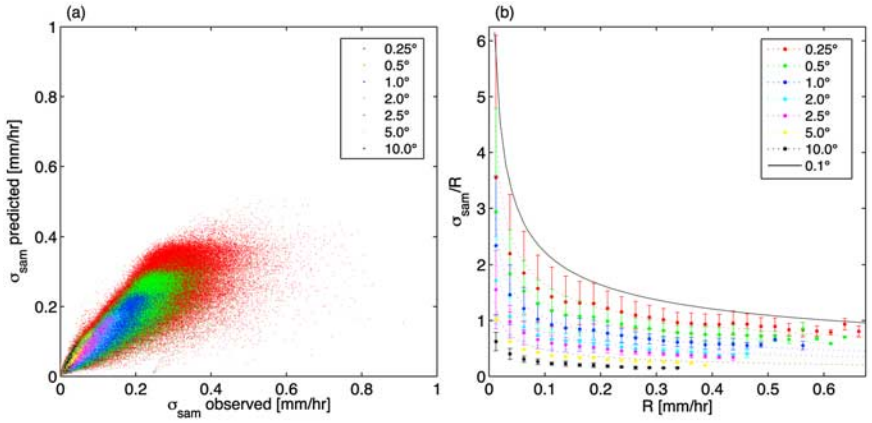

Figure 3. (a) Scatter plot of observed sampling error versus predicted sampling error from equation (3) at resolutions indicated by the colored dots. (b) Observed fractional sampling error as a function of observed rain rate (dots), dotted curves indicate predicted values as a function of resolution according to equation (3). The solid line indicates the predicted fractional sampling error at 0.1°.

masking (and extrapolation of the lowest meteorological echo to "near surface", typically a distance of 1–2 km AGL), as well as sidelobe return lead to PR retrieval error (in complex terrain in particular). However, when considering PR precipitation climatologies at very high resolution, sampling errors, due to the discontinuous and infrequent nature of measurements, are likely to be much larger than measurement errors due to the small number of samples at each location [*Anders et al.*, 2006]. A study of four years of 2A25 data in the southeastern Himalaya suggest that ground clutter, may be present in data taken at the highest look angles (>13.5 degrees), but that it does not dominate the precipitation patterns measured [*Anders et al.*, 2006].

4.2. Sampling Error

[12] Prior work predicts sampling error for satellite rainfall studies based on assumptions about the probability distribution of rain rates and the independence of sequential observations of rain rate [e.g., *Bell and Kundu*, 2000]. We present an empirical approach for estimating sampling error similar to *Steiner et al.* [2003]. We assume that the 3-hourly 3B42 combined product represents the precipitation climatology with very little sampling error relative to the TRMM PR. To simulate the sampling error in the PR-based climatology, we sub-sample the 3B42 data by "flying" the PR through 3B42, counting a 3B42 pixel as observed by the PR within each 3-hr period if more than half of the 0.25° grid box was sampled by the PR. We then degraded the 0.25° full and temporally subsampled monthly rainfall estimates to spatial resolutions of 10°, 5°, 2.5°, 2°, 1°, and 0.5°. The simulated PR climatologies are then compared to the complete 3B42 climatology to estimate sampling error at each of the seven spatial resolutions using the method of *Fisher* [2007], where

$$\sigma^2_{\text{sam}} = \sigma^2_{\text{3B42}} + \sigma^2_{\text{3B42|2A25}} - 2\text{cov}\left(\sigma^2_{\text{3B42}}, \sigma^2_{\text{3B42|2A25}}\right). \quad (1)$$

We then extrapolate from the relationship between resolution and error to estimate error at the 0.1° resolution of our 10-year 2A25 precipitation climatology. To do this we need to assume that the space-time scaling properties of rainfall are consistent across the resolutions considered.

[13] *Steiner et al.* [2003] and *Iida et al.* [2006] fit a power law to subsampled ground-based rainfall estimates to equations of the form

$$\sigma_{\text{sam}} = aR^bA^cF^d. \quad (2)$$

Similarly, we fit a power-law model where σ_{sam} is the sampling error, a is a constant depending on rain rate R in mm/hr, grid resolution A in km^2, and relative sampling frequency F to the estimated sampling error. The effect of non-uniform sampling as a function of latitude is accounted for by defining the relative frequency of sampling F for each grid resolution as the number of samples taken at each latitude divided by the maximum number of samples taken in any grid box at that resolution.

[14] Using estimated error at all resolutions, we find the coefficients (with 95% confidence intervals) on equation (2) to be $a = 0.77 \pm 0.007$, $b = 0.56 \pm 0.001$, $c = -0.33 \pm 0.001$, and $d = -0.55 \pm 0.003$, with an r^2 value of 0.82 (Figure 3a). Considering the data at each resolution and fixing A and F at the median values for each resolution reveals that relative error is overestimated at smaller rain rates and for coarser resolution (Figure 3b). A weighted regression accounting for the disparate sample sizes at each resolution, as well as separate power law fits to the dependence of error on resolution did not improve the r^2 of the model fit. The lack of coherence in rain-rate vs. error relationship across scales as well as decreasing model performance at resolutions coarser than 1° supports the idea that there may be a change in power-law scaling with resolution around this value, which was also found by *Iida et al.* [2006]. Detailed consideration of the structure of the errors, including the spatiotemporal structure of the errors, influence of comparing instantaneous PR measurements and 3 hr 3B42 estimates, and the non-trivial relationship between error and resolution found herein, are subject to further research. Nevertheless, we conclude that, at higher rain rates, the relative error decreases with rain rate, to the point where errors at 0.1° resolution decrease below 100% at around 0.4

mm/h (9.6 mm/day). As an illustration, estimated sampling errors for South America and South Asia are shown in Figures 1d and 1e.

5. Conclusions

[15] The 10-yr precipitation climatology produced from TRMM 2A25 data provides a unique view into orographic precipitation processes in tropical mountain ranges, and is suitable for studies of landscape evolution. Sampling errors are certainly still significant, even after ten years of data collection. More data will decrease these errors: a doubling of the period of record is equivalent to a halving of the error variance at a fixed resolution. In regions with large gradients in precipitation, however, the current climatology is sufficient to resolve important spatial gradients. Despite the large errors predicted at high resolution, in regions with large precipitation totals (>12 mm/day or 0.5 mm/h) and large gradients in precipitation (e.g., Figures 1b and 1c), sampling error is small enough to define statistically significant precipitation differences. However, several important caveats are necessary. Firstly, sampling errors are significant and need to be considered for each particular application, and likely depend on rainfall properties. Secondly, complex terrain presents several specific challenges for satellite precipitation radar including unique measurement and retrieval errors. Finally, higher-latitude regions are dominated by smaller precipitation totals and more frequent occurrence of frozen precipitation, adding to the challenges of satellite precipitation radar measurements. These issues will become more crucial for the planned Global Precipitation Mission (GPM), which will sample high-latitude orographic precipitation regimes.

[16] **Acknowledgments.** We acknowledge excellent comments from two anonymous reviewers. Data were obtained from the NASA GES DISC. SN was supported by the NASA New Investigator Program in Earth System Science (grant NNX08AQ85G). The PR climatology is available at http://www.atmos.illinois.edu/precip.

References

Anders, A. M., G. H. Roe, B. Hallet, D. R. Montgomery, N. J. Finnegan, and J. Putkonen (2006), Spatial patters of precipitation and topography in the Himalaya, in *Tectonics, Climate, and Landscape Evolution*, edited by S. D. Willett et al., pp. 39–53, Geol. Soc. of Am., Boulder, Colo.

Barros, A. P., G. Kim, E. Williams, and S. W. Nesbitt (2004), Probing orographic controls in the Himalayas during the monsoon using satellite imagery, *Nat. Hazards Earth Syst. Sci.*, *4*, 29–51.

Bell, T. L., and P. K. Kundu (1996), A study of the sampling error in satellite rainfall estimates using optimal averaging of data and a stochastic model, *J. Clim.*, *9*, 1251–1268, doi:10.1175/1520-0442(1996)009<1251:ASOTSE>2.0.CO;2.

Bell, T. L., and P. K. Kundu (2000), Dependence of satellite sampling error on monthly averaged rain rates: Comparison of simple models and recent studies, *J. Clim.*, *13*, 449–462, doi:10.1175/1520-0442(2000)013<0449:DOSSEO>2.0.CO;2.

Bilanow, S., and S. Slojkowski (2006), TRMM on-orbit performance reassessed after control change, paper presented at 19th International Symposium on Space Flight Dynamics, Jpn. Aerosp. Explor. Agency, Kanazawa, Japan.

Bookhagen, B., and D. W. Burbank (2006), Topography, relief, and TRMM-derived rainfall variations along the Himalaya, *Geophys. Res. Lett.*, *33*, L08405, doi:10.1029/2006GL026037.

Bookhagen, B., and M. R. Strecker (2008), Orographic barriers, high-resolution TRMM rainfall, and relief variations along the eastern Andes, *Geophys. Res. Lett.*, *35*, L06403, doi:10.1029/2007GL032011.

Daly, C., R. P. Neilson, and D. L. Phillips (1994), A statistical topographic model for mapping climatological precipitation over mountainous terrain, *J. Appl. Meteorol.*, *33*, 140–158, doi:10.1175/1520-0450(1994)033<0140:ASTMFM>2.0.CO;2.

Fisher, B. L. (2007), Statistical error decomposition of regional-scale climatological precipitation estimates from the Tropical Rainfall Measuring Mission (TRMM), *J. Appl. Meteorol. Climatol.*, *46*, 791–813, doi:10.1175/JAM2497.1.

Grossman, R. L., and D. R. Durran (1984), Interaction of low-level flow with the Western Ghat Mountains and offshore convection in the summer monsoon, *Mon. Weather Rev.*, *112*, 652–672, doi:10.1175/1520-0493(1984)112<0652:IOLLFW>2.0.CO;2.

Haddad, Z. S., E. A. Smith, C. D. Kummerow, T. Iguchi, M. R. Farrar, S. L. Durden, M. Alves, and W. S. Olson (1997), The TRMM "day-1" radar/radiometer combined rain-profiling algorithm, *J. Meteorol. Soc. Jpn.*, *75*, 799–809.

Huffman,G.J.,R.F.Adler,D.T.Bolvin,G.Gu,E.J.Nelkin,K.P.Bowman,Bowman, Bowman, Y. Hong, E. F. Stocker, and D. B. Wolff (2007), The TRMM Multisatellite Precipitation Analysis (TMPA): Quasi-global, multiyear, combined-sensor precipitation estimates at fine scales, *J. Hydrometeorol.*, *8*, 38–55, doi:10.1175/JHM560.1.

Iguchi, T., T. Kozu, R. Meneghini, J. Awaka, and K. Okamoto (2000), Rain-profiling algorithm for the TRMM precipitation radar, *J. Appl. Meteorol.*, *39*, 2038–2052, doi:10.1175/1520-0450(2001)040<2038:RPAFTT>2.0.CO;2.

Iida, Y., K. Okamoto, T. Ushio, and R. Oki (2006), Simulation of sampling error of average rainfall rates in space and time by five satellites using radar-AMeDAS composites, *Geophys. Res. Lett.*, *33*, L01816, doi:10.1029/2005GL024910.

Kidd, C., and G. R. McGregor (2007), Observation and characterisation of rainfall over Hawaii and surrounding region from the Tropical Rainfall Measuring Mission, *Int. J. Climatol.*, *27*, 541–553, doi:10.1002/joc.1414.

Mapes, B. E., T. T. Warner, M. Xu, and A. J. Negri (2003), Diurnal patterns of rainfall in northwestern South America. Part I: Observations and context, *Mon. Weather Rev.*, *131*, 799–812, doi:10.1175/1520-0493(2003)131<0799:DPORIN>2.0.CO;2.

Ogura, Y., and M. Yoshizaki (1988), Numerical study of orographic-convective precipitation over the eastern Arabian Sea and the Ghat Mountains during the summer monsoon, *J. Atmos. Sci.*, *45*, 2097–2122, doi:10.1175/1520-0469(1988)045<2097:NSOOCP>2.0.CO;2.

Rosenfeld, D., and C. W. Ulbrich (2003), Cloud microphysical properties, processes, and rainfall estimation opportunities, *Meteorol. Monogr.*, *30*, 237, doi:10.1175/0065-9401(2003)030<0237:CMPPAR>2.0.CO;2.

Smith, R. B. (1985), Comment on "Interaction of low-level flow with the Western Ghat Mountains and offshore convection in the summer monsoon," *Mon. Weather Rev.*, *113*, 2176–2177, doi:10.1175/1520-0493(1985)113<2176:COOLLF>2.0.CO;2.

Steiner, M., T. L. Bell, Y. Zhang, and E. F. Wood (2003), Comparison of two methods for estimating the sampling-related uncertainty of satellite rainfall averages based on a large radar dataset, *J. Clim.*, *16*, 3759–3778, doi:10.1175/1520-0442(2003)016<3759:COTMFE>2.0.CO;2.

Xie, S. P., H. M. Xu, N. H. Saji, Y. Q. Wang, and W. T. Liu (2006), Role of narrow mountains in large-scale organization of Asian monsoon convection, *J. Clim.*, *19*, 3420–3429, doi:10.1175/JCLI3777.1.

A. M. Anders, Department of Geology, University of Illinois at Urbana-Champaign, 253 Natural History Building, 1301 West Green Street, Urbana, IL 61801, USA.

S. W. Nesbitt, Department of Atmospheric Sciences, University of Illinois, 105 South Gregory Street, Urbana, IL 61801, USA. (snesbitt@illinois.edu)